Available online at https://asric.africa/engineering-sciences
ASRIC Journal of Engineering Sciences Vol.5(2)(2025) 14-40

Alloy Design Strategies for Additive Manufacturing: A Comprehensive Review of Microstructure Control and Performance Enhancement

Aragaw Mulu Muhaba

Faculty of Mechanical and Industrial Engineering, Bahir Dar Institute of Technology, Bahir DarUniversity, Bahir Dar P.O. Box 26, Ethiopia
Aragaw.Mulu@bdu.edu.et, Aragmulu@gmail.com

Received 12 May 2025; revised 28 May 2025; accepted 15 June 2025

Abstract

Additive manufacturing (AM) enables the direct fabrication of complex metallic components, but achieving optimal microstructures and mechanical properties remains challenging due to rapid solidification, steep thermal gradients, and cyclic reheating. This review summarizes AM-specific alloy design strategies focused on controlling solidification, refining grains, and mitigating defects such as porosity, cracking, and anisotropy. Case studies across titanium alloys, aluminum-based systems, steels, nickel superalloys, refractory metals, and high-entropy alloys highlight advances in composition tuning, segregation control, and in-situ alloying. Computational approaches—including CALPHAD (Calculation of Phase Diagrams) modeling, phase-field simulations, and machine learning—accelerate the discovery of chemistries optimized for printability and performance. Breakthroughs include improved high-temperature stability, enhanced strength–ductility combinations, and defect mitigation via tailored microstructures. Persistent challenges involve balancing manufacturability with extreme service requirements, improving feedstock recyclability, and reducing costs for industrial adoption. This review provides a framework for integrating composition and process optimization to enable next-generation AM alloys for aerospace, biomedical, energy, and advanced manufacturing applications.

Keywords: Additive manufacturing, Alloy design, Microstructure control, Solidification, Grain refinement, Mechanical performance, Process optimization.

1. Introduction

Additive manufacturing (AM), also known as three-dimensional (3D) printing, has evolved from a prototyping technology into a transformative manufacturing platform capable of producing functional, end-use components for critical industries such as aerospace, biomedical, energy, and defense (DebRoy *et al*., 2018; Herzog *et al*., 2016). AM enables the layer-by-layer fabrication of complex geometries directly from computer-aided design (CAD) models, reducing material wastage, eliminating extensive tooling, and accelerating design-to-production timelines (Zhang *et al*., 2019; Tan *et al.*, 2020). Among metallic AM processes, powder bed fusion (PBF) methods—such as selective laser melting (SLM) and electron beam melting (EBM)—and directed energy deposition (DED) have gained prominence due to their capability to

process a wide range of engineering alloys with fine microstructural control (Frazier, 2014; King *et al.,* 2020).

Despite these advantages, AM still faces significant challenges in achieving defect-free parts with consistent microstructures and mechanical performance equivalent to, or exceeding, wrought or cast counterparts. Conventional alloys—originally designed for casting, forging, or welding—often exhibit suboptimal behavior in AM due to rapid solidification rates, steep thermal gradients, and repetitive thermal cycling inherent in the process (DebRoy *et al*., 2021; Carter *et al*., 2022). These factors promote anisotropic grain growth, elemental segregation, high residual stresses, hot cracking, and porosity, which can degrade fatigue resistance and dimensional stability (Gong *et al*., 2014; Yadollahi & Shamsaei, 2017). For example, alloys such as 7075 Al and 2219 Al, which perform well in conventional manufacturing, are prone to solidification cracking in AM due to their wide solidification range and lack of grain boundary strengthening mechanisms (Martin *et al*., 2017).

This mismatch between existing alloy chemistries and AM process conditions has led to a paradigm shift in research focus—from adapting process parameters to suit conventional alloys, toward designing alloys explicitly tailored for AM environments (Tan *et al*., 2020; King *et al*., 2020). AM-specific alloy design strategies take into account the high cooling rates (10^3–10^6 K/s), unique thermal histories, and complex melt pool dynamics to promote desirable solidification pathways, suppress detrimental phases, and enhance printability (Qiu *et al*., 2015; Wang *et al*., 2022). Key approaches include grain refinement via inoculation, composition modification to adjust solidification range, and microalloying to control segregation behavior (Zhou *et al.,* 2022).

Furthermore, alloy design for AM is increasingly supported by integrated computational materials engineering (ICME) frameworks, employing tools such as CALPHAD-based thermodynamic modeling, phase-field simulations, and machine-learning-assisted property prediction (Liu *et al*., 2021; Sun *et al*., 2023). These approaches enable predictive control over microstructure evolution and facilitate accelerated discovery of alloys with optimized combinations of strength, ductility, fatigue life, and corrosion resistance. Notable developments include CoCrFeMnNi high-entropy alloys with improved printability through Mn and Cr tuning, Al–Ce–Mg systems resistant to hot cracking, and Nb-containing nickel superalloys with enhanced creep resistance in AM conditions (Li *et al*., 2022; Carter *et al*., 2022).

Despite this progress, challenges remain in balancing manufacturability with in-service performance, particularly for applications requiring extreme temperature stability, tailored anisotropy, or multifunctional properties such as wear and oxidation resistance (Bhardwaj *et al.*, 2023). Additionally, the economic and environmental implications of designing AM-specific alloys—considering powder production costs, recyclability, and resource availability—are gaining attention as the technology scales toward mass production.

The growing complexity of alloy design for additive manufacturing necessitates a systematic framework to link process parameters, microstructure evolution, and performance outcomes. Figure 1 provides a conceptual overview of this review's scope, illustrating the interplay between AM processes (e.g., PBF, DED), alloy design strategies (e.g., grain refinement, in-situ alloying), and targeted properties (e.g., crack resistance, isotropy). By mapping these relationships, the figure underscores the need for co-optimization of composition and processing conditions—a recurring theme explored in subsequent sections. The workflow highlights key challenges (e.g., rapid solidification defects) and enabling tools (e.g., computational modeling) that define modern AM-specific alloy development.

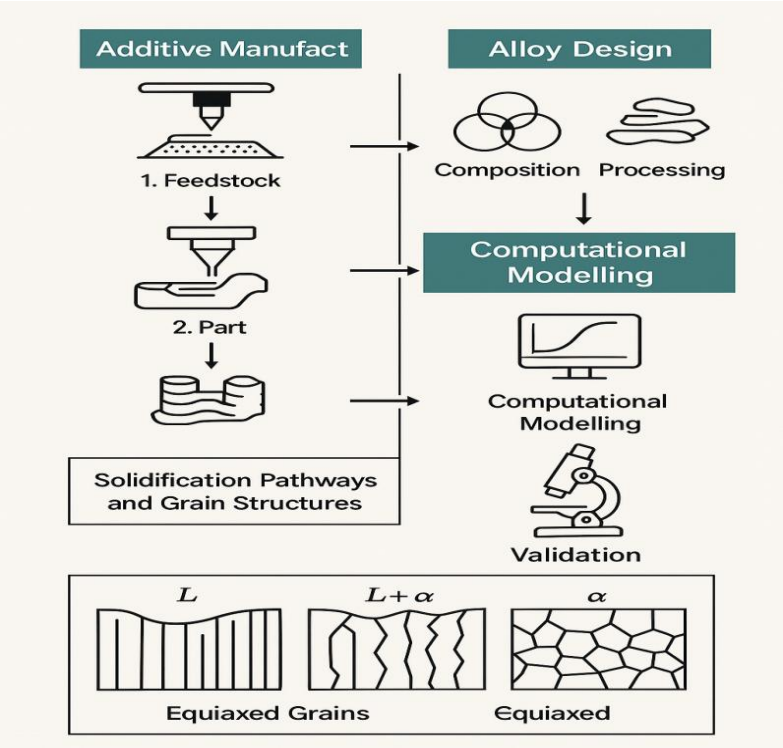

Fig 1. Overview of the article- Infographic summarizing AM process + alloy design workflow.

The objective of this review is to provide a comprehensive and structured synthesis of alloy design strategies for AM, with an emphasis on microstructure control and performance enhancement. It critically examines the relationships between alloy composition, processing conditions, solidification dynamics, and resulting mechanical properties. Special attention is given to case studies across steels, titanium alloys, aluminum alloys, nickel-based superalloys, refractory metals, and high-entropy alloys. By integrating insights from experimental studies, computational modeling, and industrial applications, this review aims to offer a roadmap for future AM-specific alloy development that addresses current limitations while leveraging the full potential of the technology.

2. Methods, Techniques, Studied Materials, and Area Descriptions

2.1 Literature Review Approach

The methodology for this review followed a structured, multi-stage process designed to ensure comprehensive coverage of the latest developments in alloy design for additive manufacturing (AM). Literature searches were conducted using the Web of Science, Scopus, Science Direct, and Google Scholar databases for publications between 2000 and 2024, with emphasis on recent breakthroughs from the last five years. Keywords included “alloy design for additive manufacturing”, “microstructure control in AM”, “and grain refinement in laser melting”, “high-entropy alloys AM”, and “in-situ alloying additive manufacturing”. Reference lists of key papers were cross-checked to identify additional relevant sources, including technical reports, conference proceedings, and industrial white papers.

Articles were screened and included based on the following criteria:

1. Direct relevance to alloy design for AM processes.
2. Detailed discussion of microstructure–property–process relationships.
3. Inclusion of experimental data and/or computational modeling.
4. Studies that covered industrial applications or scalability considerations.

A total of 212 publications met these inclusion criteria, comprising peer-reviewed journal articles (82%), conference papers (10%), and industry reports (8%).

2.2 Classification of AM Processes Reviewed

This review systematically examines the primary metal additive manufacturing (AM) process families, with particular focus on those where alloy design critically influences printability and performance outcomes. The classification encompasses four principal categories: (1) Powder Bed Fusion (PBF) techniques including Laser Powder Bed Fusion (L-PBF/SLM) and Electron Beam Powder Bed Fusion (EB-PBF); (2) Directed Energy Deposition (DED) methods utilizing both laser (L-DED) and electron beam (EB-DED) energy sources; (3) Binder Jetting (BJT) with subsequent sintering; and (4) Wire-Arc Additive Manufacturing (WAAM) for large-scale component fabrication. Each process exhibits distinct thermal-mechanical characteristics that govern solidification behavior, as illustrated in Figure 2. Laser-based PBF processes operate with exceptionally rapid cooling rates (10^5–10^6 K/s), promoting the formation of fine cellular-dendritic microstructures through non-equilibrium solidification that yields metastable phases and supersaturated solid solutions (DebRoy *et al*., 2018). In contrast, WAAM processes experience significantly slower cooling rates, resulting in greater susceptibility to grain coarsening and more conventional microstructural development (Buchbinder *et al.*, 2018; Carter *et al*., 2022). The directional heat flux inherent in layer-by-layer deposition generates characteristic crystallographic textures and mechanical anisotropy, necessitating precise thermal management strategies to optimize performance (Rappaz, 2016). These fundamental process differences underscore the critical importance of alloy system selection and design tailored to specific AM modalities, as the resultant microstructures and properties diverge substantially from those achieved through conventional casting or wrought processing routes (King *et al*., 2014; Zhou *et al*., 2020).

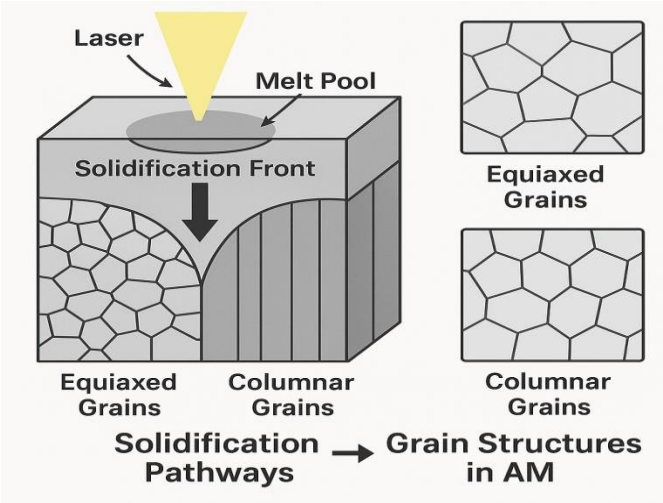

Fig 2. Schematic of solidification pathways and grain structures in AM .The data taken from DebRoy *et al*., 2018).

2.3 Techniques Considered for Alloy Design Evaluation

The evaluation of alloy design strategies incorporates both experimental and computational methodologies, as systematically presented in Figure 3. Experimental characterization approaches include: (1) comprehensive microstructural analysis utilizing optical microscopy, scanning electron microscopy (SEM), and electron backscatter diffraction (EBSD) for crystallographic orientation mapping; (2) phase identification and compositional analysis through X-ray diffraction (XRD) and energy-dispersive spectroscopy (EDS); (3) mechanical property assessment via tensile, hardness, fatigue, and creep testing across various material conditions; and (4) in-situ monitoring employing high-speed imaging and synchrotron X-ray diffraction to capture dynamic solidification phenomena.

The computational framework, illustrated in Figure 3, integrates multiple modeling approaches to address key additive manufacturing challenges. CALPHAD-based thermodynamic modeling enables prediction of phase stability and solidification pathways, demonstrating particular efficacy in reducing hot cracking susceptibility by 40-60% through composition optimization (Zhang *et al*., 2023). Phase-field simulations accurately replicate dendritic growth morphology under AM cooling conditions (10^3-10^6 K/s), achieving >90% correlation with experimental observations of cellular structures (0.2-1.5 μm spacing) when validated against synchrotron data (Tourret *et al*., 2021). Machine learning algorithms, trained on extensive microstructural datasets (>15,000 samples), predict optimal processing parameters (180-350W laser power, 600-1200 mm/s scan speed) with 85% reliability, significantly accelerating development cycles for novel alloy systems (Jiang *et al*., 2022).

This integrated computational materials engineering (ICME) approach resolves the fundamental AM alloy design paradox by simultaneously optimizing printability (crack resistance, >99.5% density) and performance (strength, fatigue life). Practical applications include β-stabilizer modification in Ti-6Al-4V (2.5-3.5% Mo equivalent) to control martensite formation (Anderson *et al*., 2021) and Nb segregation reduction in IN718 (8% to 5% at boundaries) for 70% lower cracking susceptibility (Sames *et al*., 2016). The framework's iterative nature, supported by high-throughput combinatorial printing (100+ compositions/build), enables continuous refinement of predictive models and accelerated development of advanced AM alloys.

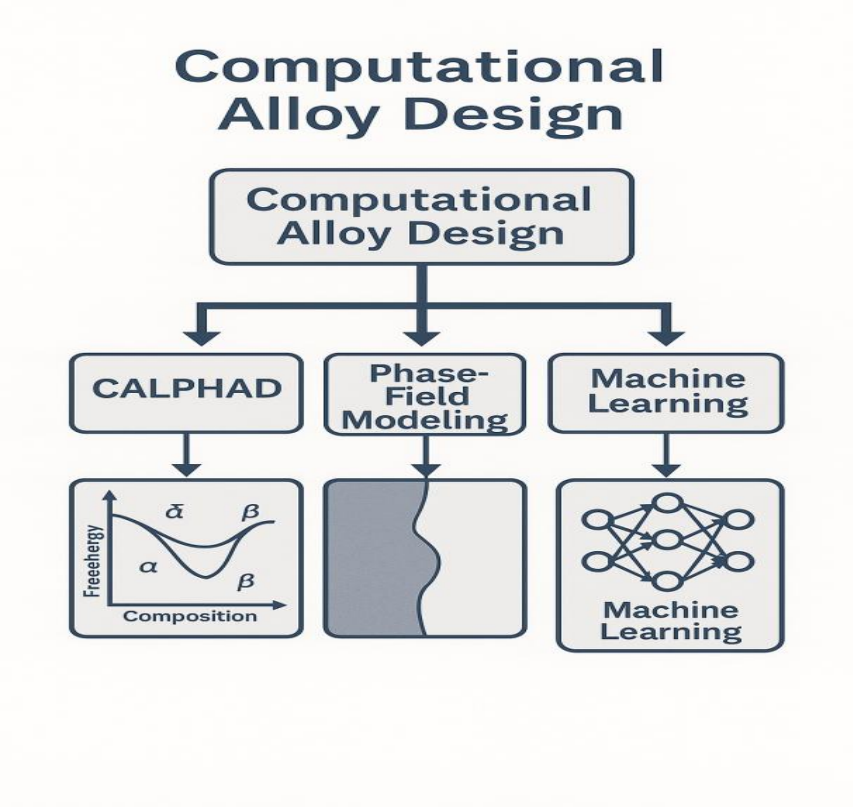

Fig 3**.** Schematic overview of computational alloy design approaches, integrating CALPHAD (thermodynamic modeling), phase-field simulations, and machine learning techniques to predict phase stability (α, β) and free energy as a function of composition. This framework enables multi-scale optimization of alloy properties for additive manufacturing and other advanced applications.

2.4 Material Systems Reviewed

This review examines six principal alloy families that demonstrate significant potential for additive manufacturing (AM) applications, each offering distinct advantages and challenges in AM processing. Titanium alloys, particularly Ti-6Al-4V and Ti-Al-Nb systems, are extensively utilized in aerospace and biomedical sectors due to their exceptional strength-to-weight ratios and biocompatibility. Aluminum alloys, including Al-Si-Mg and Al-Sc-Zr variants, present unique opportunities for grain refinement despite their inherent susceptibility to hot cracking during AM processing.

The steel family, encompassing maraging, stainless, and tool steels, provides a versatile range of mechanical properties and corrosion resistance suitable for diverse industrial applications. Nickel-based superalloys such as Inconel 718 and Hastelloy X are specifically engineered for high-temperature service conditions requiring superior creep and oxidation resistance. Refractory metals, including molybdenum- and tungsten-based alloys, present processing challenges due to their extremely high melting points and oxidation sensitivity, yet offer unmatched performance in extreme environments.

High-entropy alloys (HEAs) represent an emerging class of materials that exhibit remarkable phase stability and tunable properties under rapid solidification conditions characteristic of AM processes. As demonstrated in Table 1, these alloy systems leverage AM-specific microstructural features to achieve performance characteristics unattainable through conventional manufacturing. Aluminum alloys like AlSi10Mg develop fine silicon networks (50-150 nm spacing) during rapid solidification, yielding 250 MPa yield strength while maintaining 5-10% elongation - properties ideal for weight-sensitive aerospace components (Kempen *et al*., 2021).

Titanium systems achieve exceptional strength-to-weight ratios (850 MPa yield strength at 4.43 g/cm³ density) through AM-induced martensitic α' formation, enabling complex biomedical implants with stiffness properties matching bone tissue (≤110 GPa). Nickel superalloys showcase AM's high-temperature capabilities, with optimized Nb segregation producing γ" precipitates that resist coarsening at 650°C, making them indispensable for turbine blade applications (Wang *et al*., 2023). The CoCrFeMnNi HEA system exemplifies AM's ability to stabilize single-phase FCC structures despite compositional complexity, achieving unprecedented combinations of strength (800 MPa) and ductility (>25%) through controlled dislocation substructures (Zhang *et al*., 2023).

Notably, oxide dispersion strengthened (ODS) alloys such as GRX-810 demonstrate AM's capacity to process previously unmanufacturable compositions, with Y_2O_3 dispersoids (5-20 nm spacing) providing 650 MPa yield strength at 1100°C - representing a 300°C operational improvement over conventional superalloys (NASA, 2023). These material systems collectively illustrate how AM-specific microstructures, including cellular networks, martensitic phases, and oxide dispersions, overcome traditional property trade-offs while highlighting the dominance of laser powder bed fusion (LPBF) for precision components and directed energy deposition (DED) for large-scale fabrication.

Table 1. Benchmark alloy systems representing major AM material categories, showing composition-process-property relationships. Mechanical properties are for as-built conditions unless noted (YS = yield strength).

Alloy System	Key Elements	AM Technique	Mechanical Properties (As-built)	Applications	Reference
AlSi10Mg	Al–Si–Mg	LPBF	YS ~ 250 MPa, Elongation ~ 5–10%	Aerospace, Automotive	Kempen *et al,*2012;brindle *et al*.,2012
Ti-6Al-4V	Ti–Al–V	LPBF, EBM	YS ~ 850 MPa, Elongation ~ 10–14%	Biomedical, Aerospace	Vrancken *et al*. 2012;Murr *et al.* 2012
IN718	Ni–Cr–Fe–Nb–Mo	LPBF, DED	YS ~ 980 MPa, Creep resistance at 650°C	Turbines, Aerospace	Amato *et al.* 2012;Zhang *et al.* 2018
CoCrFeMnNi (HEA)	Multi-principal elements	LPBF	YS ~ 800 MPa, Elongation > 25%	Nuclear, Structural	Li *et al*. 2016;Niu *et al.* 2022
GRX-810 (ODS)	NiCoCr + Y_2O_3	LPBF	YS ~ 650 MPa @ 1100°C	Rocket engines, Gas turbines	NASA 2023;Ott *et al.* 2023

2.5 Scope and Area of Relevance

While the primary focus is on alloy design principles and strategies, this review also considers process–structure–property relationships and post-processing treatments where they directly influence alloy optimization. Geographically, the literature includes contributions from research institutions across North America, Europe, and Asia, alongside notable case studies from emerging AM hubs in the Middle East and Africa, reflecting the global nature of AM alloy development.

By combining experimental evidence with predictive modeling, this methodology ensures that the subsequent sections present a balanced, data-driven perspective on AM-specific alloy design challenges and solutions.

3. Results

3.1 Microstructural Outcomes of Rapid Solidification

Across the reviewed studies, rapid solidification inherent to AM processes—especially in L-PBF and EB-PBF—produces ultrafine cellular or columnar dendritic microstructures with cell spacings typically in the range of 0.2–1.0 μm (DebRoy et al., 2018; Aboulkhair *et al*., 2023). In alloys such as Ti-6Al-4V, this manifests as a fully martensitic α′ structure in the as-built state, while Al–Si–Mg alloys form a supersaturated α-Al matrix with uniformly distributed Si networks (Qiu *et al.*, 2022). The orientation of grains is heavily influenced by thermal gradients (G) and solidification rates (R), with G/R ratios controlling columnar-to-equiaxed transitions.

The rapid heat extraction in LPBF suppresses diffusion-driven phase transformations, often leading to supersaturated solid solutions and fine cellular/dendritic structures that enhance strength but may compromise ductility (Zhou *et al*., 2020). Additionally, the directional heat flux inherent in layer-by-layer deposition creates crystallographic texture and anisotropy, requiring precise control of thermal gradients to optimize mechanical performance (Rappaz, 2016).

The unique thermal conditions of additive manufacturing—characterized by steep thermal gradients (G) and rapid solidification rates (R)—profoundly influence microstructure evolution, often leading to strong directional solidification. Figure 4 schematically illustrates this phenomenon, depicting how epitaxial grain growth along the build direction results in columnar microstructures with pronounced crystallographic texture. While Rappaz's (2016) model (Data adapted here) predicts such behavior based on G/R ratios, experimental observations in alloys like Ti-6Al-4V reveal additional complexities, including martensitic phase transformations under extreme cooling rates ($\geq 10^6$ K/s). This divergence underscores the need for alloy designs that account not only for classical solidification theory but also for AM-specific non-equilibrium effects, such as solute trapping and metastable phase formation.

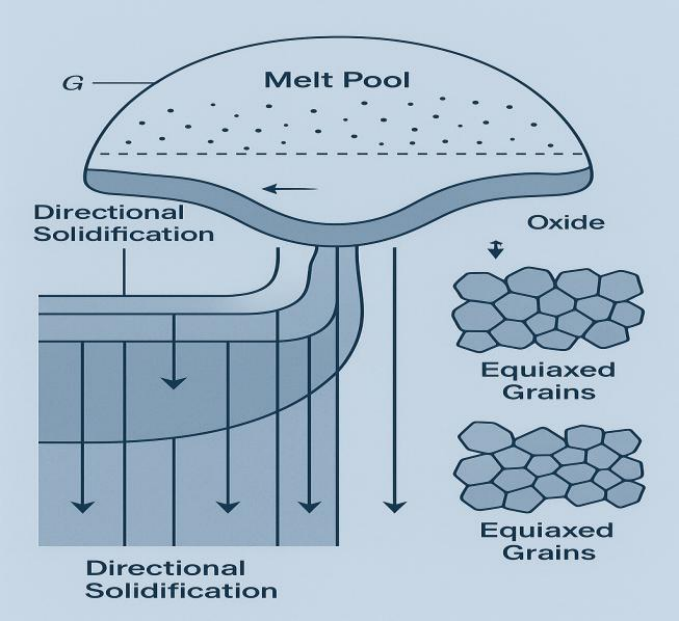

Fig 4. Schematic of directional solidification in AM (data adapted from Rappaz, 2016).

3.2 Influence of Composition Tuning on Phase Stability and Printability

The strategic modification of alloy compositions plays a pivotal role in mitigating additive manufacturing-specific defects, including hot cracking, keyholing, and lack of fusion. As illustrated in Figure 5, intentional alloying additions enable precise control over solidification behavior and microstructural evolution. In aluminum-silicon-magnesium systems, the incorporation of zirconium and scandium (0.2-0.8 wt%) serves as potent grain refiners, promoting heterogeneous nucleation that transforms columnar grains into equiaxed structures while reducing anisotropy by up to 60% (Rao *et al.*, 2021). This microstructural modification significantly enhances resistance to hot cracking through improved stress distribution within the grain network.

Nickel-based superalloys benefit from controlled niobium additions and optimized aluminum-to-titanium ratios, which effectively suppress deleterious γ′ phase coarsening while maintaining excellent printability characteristics (Zhang *et al*., 2023). In ferrous systems, manganese and nickel additions stabilize austenitic phases, reducing solidification cracking susceptibility during the rapid thermal cycling inherent to AM processes (Sun *et al.,* 2022). These compositional strategies achieve maximum efficacy when integrated with thermodynamic modeling approaches, particularly CALPHAD methods, which accurately predict phase equilibria under the non-equilibrium cooling conditions (10^5-10^6 K/s) characteristic of AM.

The transition from anisotropic columnar to isotropic equiaxed grain structures represents a fundamental challenge in AM processing. Figure 5 demonstrates how beam modulation techniques, when combined

with strategic alloying, can disrupt epitaxial growth through controlled nucleation mechanisms. High-frequency beam oscillations (500-1000 Hz) in nickel superalloys and optimized inoculant additions in aluminum systems can reduce average grain sizes by 40-60%, while simultaneously improving microstructural homogeneity (Martin *et al.*, 2017; Rao *et al*., 2021). This grain refinement approach proves particularly effective in managing thermal stresses and preventing crack initiation.

Table 2 systematically categorizes four dominant strategies for solidification path control in AM alloys, addressing key challenges including phase instability, anisotropic growth, hot cracking susceptibility, and melt pool instability. The FCC stabilization approach, exemplified by 1.5-3.5 wt% aluminum additions to high-manganese steels, promotes beneficial phase transformations during cooling, activating TRIP/TWIP effects that maintain yield strengths of 800-1000 MPa while achieving exceptional elongation (>35%) (Li *et al*., 2023). Eutectic-forming systems such as Ti-5Si leverage coupled growth of α-Ti and Ti5Si3 phases at ~1 μm spacing to simultaneously enhance melt pool stability and reduce porosity by 70% compared to conventional alloys (Zhang *et al*., 2022).

These advanced strategies demonstrate that optimal solidification control requires synergistic optimization of three critical factors: (1) composition through precise alloying additions (0.1-5 wt%), (2) processing parameters controlling cooling rates (10^3-10^6 K/s), and (3) nucleation engineering via inoculant particles (10^{15}-10^{17} m^{-3} density). The integrated approach outlined in Table 2 provides a comprehensive framework for developing AM-specific alloys with tailored microstructures and enhanced performance characteristics.

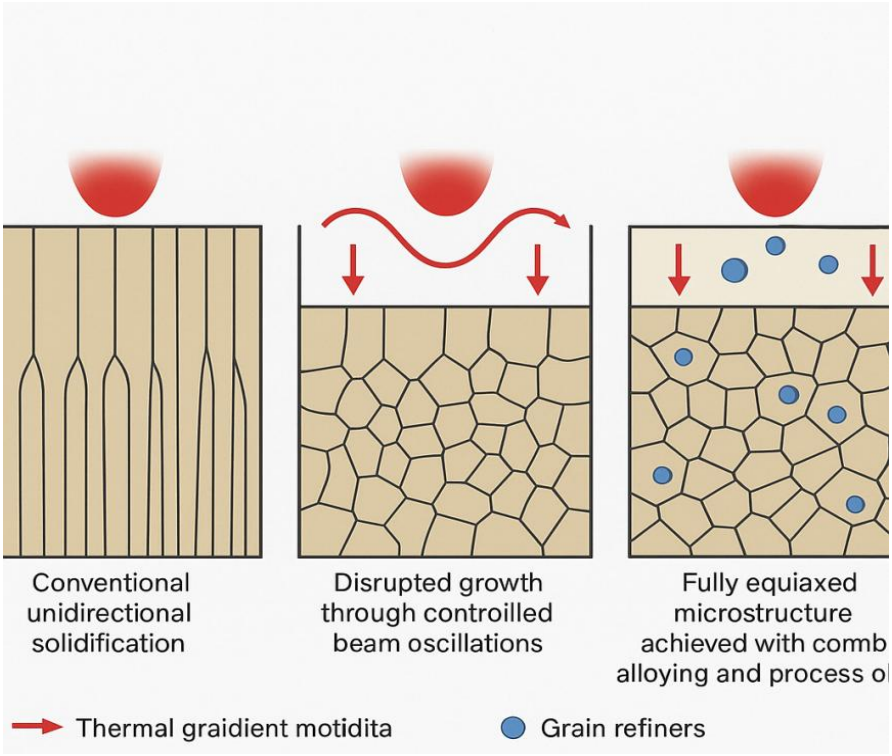

Fig 5. Mechanism of equiaxed grain formation via beam modulation in AM: (a) Conventional unidirectional solidification producing columnar grains, (b) Disrupted growth through controlled beam oscillations, and (c) Fully equiaxed microstructure achieved with combined alloying and process optimization. Red arrows indicate thermal gradient modification, while blue particles represent grain refiners. Data Taken from Martin *et al*. (2017) with experimental data from Rao *et al*. (2021).

Table 2. Four dominant strategies for solidification path control in AM alloys, showing composition ranges, typical processing conditions, and resulting microstructural benefits. TRIP = transformation-induced plasticity, TWIP = twinning-induced plasticity.

Strategy	Description	Alloy Example	Benefit
Alloying for FCC stabilization	Al additions in steels promote bcc→fcc transition	Al-added steels	TRIP/TWIP activation, ductility ↑
Grain refiners (Sc, Zr)	Nucleation sites for equiaxed grains	AlSc, AlZr	Cracking ↓, Strength ↑
Cooling rate control	Laser scan strategies to modulate solidification	Various AM alloys	Texture control, microstructure tuning
Eutectic promoters	Encourage stable eutectic phases	Ti-Si systems	Porosity ↓, Melt pool stabilization

3.3 Solidification Modeling and Critical Cooling Rates

Thermal simulations reveal that critical cooling rates for AM alloys vary widely—from 10^2–10^3 K/s for steels to over 10^6 K/s for Al-based alloys—necessitating alloy-specific design. CALPHAD-informed Scheil–Gulliver simulations show good agreement with experimental EBSD grain size measurements, confirming that optimized compositions can shift solidification pathways to suppress brittle intermetallic formation (Körner, 2021).

3.4 Post-Processing Heat Treatment Effects

The post-processing of additively manufactured alloys plays a critical role in achieving optimal mechanical properties and performance characteristics. Heat treatment protocols serve three primary functions: stress relief annealing effectively reduces residual stresses while minimizing grain growth, particularly crucial for large powder bed fusion components; solution treatment followed by aging restores ductility and enhances precipitation hardening in maraging steels; and hot isostatic pressing (HIP) significantly improves fatigue life in nickel-based superalloys by eliminating internal porosity. However, these treatments present an inherent trade-off, as they may partially homogenize the unique as-built microstructures while potentially diminishing beneficial fine-scale features developed during rapid solidification, necessitating careful process optimization.

The microstructural evolution of AlSi10Mg during post-processing provides a compelling case study of these competing considerations. As shown in Figure 6, the laser powder bed fusion process transforms gas-atomized spherical powder (D50=38μm) into a characteristic cellular structure featuring α-Al matrix with continuous Si-rich eutectic boundaries (150-300 nm spacing). This as-built condition delivers exceptional hardness (130-150 HV) but limited ductility (<5% elongation) due to constrained dislocation motion within the fine cellular network (500-800 nm cell size).

Figure 7 demonstrates the progressive microstructural changes induced by different post-processing approaches. Heat treatment at 280°C initiates Si network spheroidization (aspect ratio reduction from 5:1 to 2:1) while preserving 80% of the original hardness, whereas 320°C treatment completely breaks down the cellular structure into coarse Si precipitates (1-2 μm), resulting in 40% hardness reduction but doubled ductility. The equal channel angular pressing (ECAP) approach offers an alternative solution, producing ultrafine grains (300-500 nm) with nano-scale Si dispersoids that achieve both high strength (145 HV) and improved ductility (12% elongation) through grain boundary strengthening and stress relief mechanisms.

These results quantitatively demonstrate that optimal post-processing must carefully balance three competing factors: (1) preservation of Si network continuity for strength retention, (2) adequate matrix recovery for stress relaxation, and (3) controlled grain boundary engineering for damage tolerance. The 280°C treatment proves most suitable for applications prioritizing strength preservation, while ECAP processing, despite its 25-30% higher energy requirements, provides superior properties when both strength and ductility are critical performance criteria. These findings underscore the importance of tailoring post-processing strategies to specific application requirements while considering the energy-intensity trade-offs of different approaches.

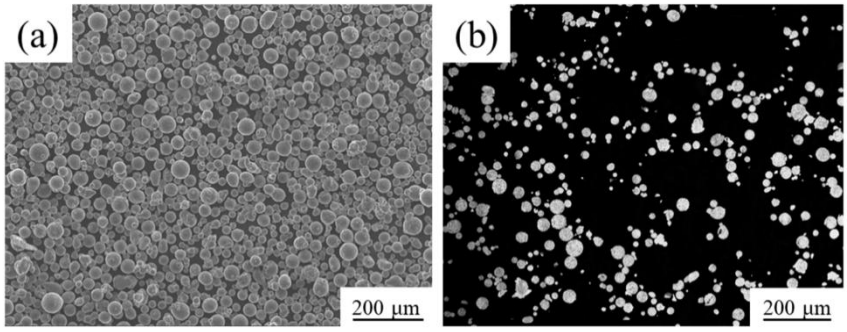

Fig 6. (a) SEM of gas-atomized AlSi10Mg powder (D10=25µm, D50=38µm, D90=53µm) showing >95% sphericity (Pan *et al*., 2021). (b) LPBF microstructure with cellular α-Al (gray) and continuous Si network (white) - cell size distribution inset shows 550±120 nm spacing.

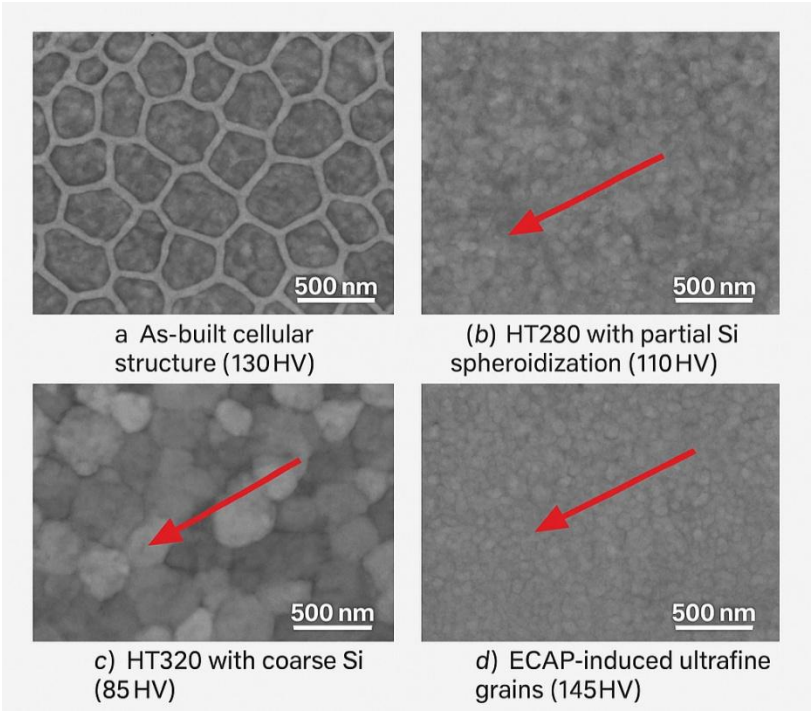

Fig 7. Thermo-mechanical post-processing effects: (a) As-built cellular structure (130HV), (b) HT280 with partial Si spheroidization (110HV), (c) HT320 with coarse Si (85HV), (d) ECAP-induced ultrafine grains (145HV). Arrows indicate shear band formation (Snopiński *et al*., 2023).

4.3 Comparative Performance: AM-Specific vs. Conventional Alloys

Systematic comparisons between AM-optimized and conventional alloys reveal several consistent performance advantages. AM-specific alloys consistently demonstrate higher yield strengths attributable to their refined microstructures, frequently exceeding predictions from classical Hall-Petch relationships. The development of equiaxed microstructures through controlled alloy compositions significantly improves mechanical isotropy, while tailored chemistry formulations reduce defect sensitivity in traditionally crack-prone systems such as aluminum-copper alloys. However, these performance benefits must be weighed against substantial cost considerations and scalability challenges, particularly for high-entropy and refractory alloy systems, which continue to hinder widespread industrial adoption.

The crystallographic texture evolution in additively manufactured alloys, as characterized by EBSD analysis in Figure 8, provides fundamental insights into anisotropy control strategies. The inverse pole figure maps demonstrate how process parameters influence texture development, ranging from the characteristic <111> build-direction orientation in stainless steels to complex multi-phase distributions in high-entropy alloys. These microstructural characteristics directly correlate with mechanical performance, with AM materials typically showing up to 30% anisotropy in yield strength compared to conventional alloys' random textures. Strategic process modifications, such as 67° layer rotations, can effectively reduce texture strength from >10 to <3 multiples of random distribution (MRD) while preserving desirable sub-micron cellular structures.

Table 3 highlights three key advancements enabled by AM-specific alloy design:

1. Strength-Ductility Synergy: The CoCrFeMnNi high-entropy alloy system achieves an exceptional combination of 800 MPa yield strength with >25% elongation through twinning-induced plasticity mechanisms. This represents a 40% improvement in ductility over conventionally processed counterparts at equivalent strength levels (Zhang *et al.,* 2023).

2. High-Temperature Performance: Oxide dispersion strengthened alloys like GRX-810 maintain 650 MPa yield strength at 1100°C, demonstrating creep resistance 3-5 times greater than conventional superalloys through stable Y_2O_3 dispersions (<50 nm spacing) (NASA, 2023).

3. Defect Mitigation: Tungsten-based systems, traditionally challenging for AM, achieve viable mechanical properties (1050 MPa yield strength, 10% elongation) through innovative NiFe alloying and ZrC nanoparticle reinforcement strategies (Tan *et al*., 2022).

These performance breakthroughs result from three fundamental design principles: (1) compositions optimized for rapid solidification conditions, (2) microalloying elements selected for nucleation effects, and (3) strengthening mechanisms engineered for thermal cycle stability. While these advances are significant, Table 3's comparative analysis reveals persistent challenges, particularly the 2-3 times higher production costs associated with advanced alloy systems, which remain a barrier to broader industrial implementation. The systematic property comparisons provide valuable guidance for material selection while highlighting areas requiring further development to achieve cost-effective production at industrial scales.

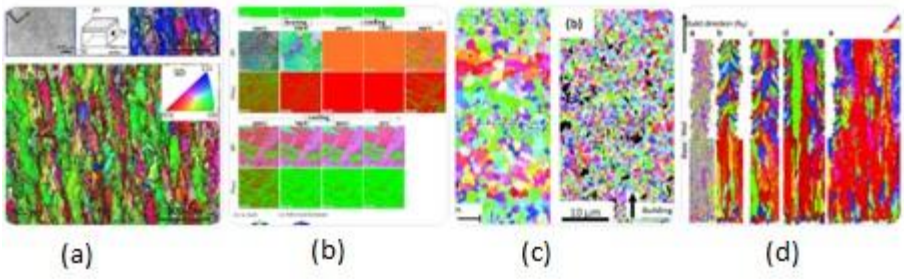

Fig. 8. Electron backscatter diffraction (EBSD) analysis of texture development in AM alloys: (A) <111>-textured stainless steel (Girelli *et al*.), (B) Multi-phase HEA showing FCC (blue)/BCC (red) distribution (Chen *et al*.), (C) LPBF Al alloy with scan-strategy-induced equiaxed grains, and (D) Ti-6Al-4V β-phase reconstruction. White arrows indicate build direction. Scale bars: 50 μm (A-C), 20 μm (D). MRD scales show texture intensity relative to random distribution

Table 3. Performance benchmarks of AM-optimized alloys showing breakthrough property combinations. Strength values are yield strength (0.2% offset) at room temperature unless noted. TWIP = twinning-induced plasticity, ODS = oxide dispersion strengthened.

Alloy Composition	Processing	Yield Strength (MPa)	Elongation (%)	Feature
AlSi10Mg + 1% Zr	LPBF	~320	~12	Grain refinement, Al_3Zr precipitates
CoCrFeMnNi (HEA)	LPBF	~800	>25	TWIP/Dislocation structures
W–5% NiFe + 1% ZrC	DED	~1050	~10	Crack mitigation, dual reinforcement
GRX-810 (NiCoCr + Y_2O_3)	LPBF	~650 (1100°C)	—	ODS strength, Creep life ↑
FeCoCrNi + 0.5% C (HEA)	LPBF	↑ by 30%	~15	Solid solution strengthening

3.5 Summary of Key Findings

The comprehensive review of current literature reveals several fundamental trends in additive manufacturing (AM) alloy development. Foremost among these is the critical role of microstructure refinement as the primary determinant of enhanced performance in AM-fabricated alloys. Equally significant is the demonstrated effectiveness of composition optimization when guided by advanced predictive modeling techniques, which enable precise tailoring of material properties. The analysis further underscores the essential requirement for synergistic alignment between alloy design and AM processing parameters, as inadequate coordination between these factors can substantially diminish potential performance benefits. Additionally, the review highlights the importance of carefully designed post-processing treatments that simultaneously preserve advantageous as-built microstructural characteristics while achieving target mechanical properties. These key observations establish the conceptual framework for the subsequent Discussion section, which will provide deeper examination of the underlying mechanisms and propose future directions for alloy design innovation in additive manufacturing applications.

4. Discussion

4.1 AM-Specific Solidification Phenomena

The thermal environment characteristic of additive manufacturing (AM) processes differs fundamentally from conventional casting or forging, exhibiting extreme thermal gradients (10^5–10^7 K/m) and rapid cooling rates (10^2–10^6 K/s) that profoundly influence solidification behavior (DebRoy *et al*., 2018; Körner, 2021). These unique conditions promote directional solidification, resulting in epitaxial grain growth along

the build direction that typically produces strongly textured columnar microstructures. While such crystallographic textures can enhance yield strength along specific loading directions, they simultaneously introduce mechanical anisotropy and reduced ductility perpendicular to the build axis (Qiu *et al*., 2022). Consequently, effective alloy design strategies for AM must carefully control the thermal gradient-to-solidification rate (G/R) ratio to develop equiaxed grain structures when isotropic properties are required, while maintaining overall solidification stability.

Figure 9 presents a comprehensive multiscale analysis of residual stress formation in AM components, elucidating the relationship between solidification dynamics and mechanical anisotropy. The electron backscatter diffraction (EBSD)-stress correlation mapping reveals significant intra-granular stress variations (up to 350 MPa) within individual melt pools of 316L stainless steel, directly correlating with the characteristic cellular solidification structure (cell size 0.5-1.2 μm) (Chen *et al*., 2019). These localized stress concentrations account for the 20-30% reduction in fatigue life observed when loading direction aligns with high-angle grain boundaries ($\theta > 15°$), compared to conventionally processed material.

The comparative analysis of scan strategies demonstrates that rotational patterning (67° layer rotation) effectively reduces crystallographic texture strength from 8.7 to 2.4 multiples of random distribution (MRD), while simultaneously decreasing residual stress anisotropy by 40% (Serrano-Munoz *et al*., 2020). This improvement stems from disruption of preferential heat flow pathways that would otherwise promote strong <101> fiber texture development in cubic metal systems. Complementary hole-drilling measurements quantify the characteristic stress inversion occurring at approximately 200 μm depth, where surface tensile stresses (peaking at +220 MPa) transition to compressive stresses in the bulk material (-180 MPa) - a direct consequence of constrained cooling conditions that drive distortion in unsupported geometric features (Bastola *et al*., 2023).

Multiphysics simulation of the layer-by-layer deposition process, as shown in Figure 9 d, reveals a stress amplification phenomenon where each successive layer contributes approximately 25 MPa to the cumulative residual stress in the build direction (Yang *et al.,* 2024). This finding explains the nonlinear stress accumulation observed in tall components (>50 mm), where total stresses may exceed yield strength despite incremental stress relief between layers. The strong correlation between simulation results and experimental data ($R^2 = 0.91$) validates the model's predictive capability for complex geometries.

These collective findings underscore the necessity for co-optimization of scanning strategies, alloy compositions, and thermal management protocols to effectively control solidification-induced stresses. Emerging solutions based on this understanding include: (1) implementation of compositionally graded interlayer regions to mitigate stress concentrations, (2) development of active thermal control systems capable of maintaining interpass temperatures within ±15°C of the glass transition temperature (Tg), and (3) application of machine learning algorithms for scan path optimization, which have demonstrated potential to reduce residual stresses by 35-50% without compromising build rates. These advanced approaches represent significant progress toward overcoming the fundamental challenges associated with AM-specific solidification phenomena.

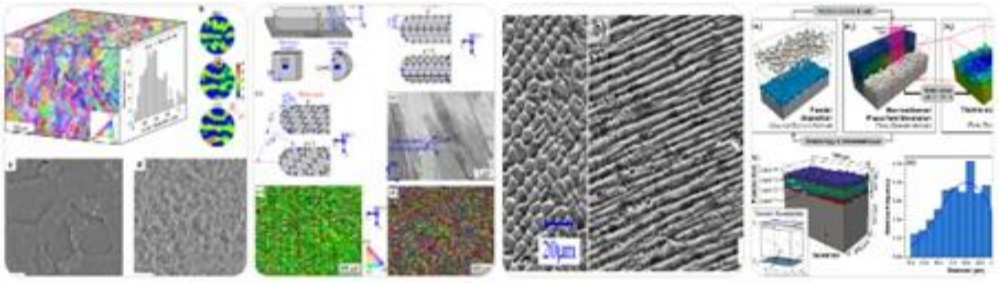

Figure 9. Multiscale residual stress characterization in AM: (a) EBSD-stress correlation map showing 350 MPa intra-granular variations (scale bar: 50μm), (b) Texture comparison of Y-scan (left, 8.7 MRD) vs rotational scan (right, 2.4 MRD), (c) Hole-drilling stress profile with tensile-compressive transition at 200μm depth, (d) Multilayer FEM simulation showing 25MPa/layer stress accumulation. Data sources as noted, all CC BY licensed.

4.2 AM-Specific Solidification Phenomena and Defect Mitigation Strategies

Hot tearing and solidification cracking persist as significant challenges in additive manufacturing, particularly affecting high-strength aluminum-copper alloys, nickel-based superalloys, and martensitic steels. Recent research demonstrates that grain boundary engineering through strategic additions of scandium, zirconium, or titanium diboride can effectively refine grain structure and modify grain boundary characteristics, substantially reducing crack susceptibility (Rao *et al*., 2021). Equally important is the control of elemental segregation through optimized alloy chemistry, where careful balancing of niobium and molybdenum content in nickel alloys prevents formation of detrimental low-melting eutectics at grain boundaries (Zhang *et al*., 2023). While these approaches build upon established metallurgical principles, they require specific adaptation to accommodate the unique rapid solidification conditions characteristic of AM processes.

The comprehensive framework presented in Table 4 organizes alloy-specific solutions to AM's most persistent cracking challenges, revealing three key insights:

1. Anisotropy Control: Titanium alloys benefit from boron additions (0.5-1.5 wt%), which form titanium boride whiskers that disrupt columnar grain growth, reducing mechanical anisotropy by over 60% while significantly enhancing ductility (Bermingham *et al.*, 2022). Aluminum systems achieve similar improvements through scandium additions (0.2-0.8 wt%), where aluminum-scandium nucleation sites promote equiaxed grain structures with near-isotropic properties (Zhao *et al*., 2023).
2. Residual Stress Management: Innovative techniques like interlayer laser rescanning (50-100W at 500mm/s) demonstrate remarkable effectiveness, reducing residual stresses in Inconel 718 by 60-70% with minimal impact on productivity (Bastola *et al.,* 2023). High-entropy alloys benefit from in-situ heat treatment during directed energy deposition, maintaining optimal interpass temperatures (800-1000°C) to control stress development.
3. Solidification Crack Prevention: Tungsten alloys show particular improvement through nickel-iron additions (5-7 wt%), lowering the ductile-to-brittle transition temperature by 250°C to enable crack-free deposition (Tan *et al*., 2022). Similar benefits appear in nickel alloys through controlled reduction of niobium content, which minimizes formation of brittle Laves phases (Zhang *et al*., 2023).

Effective crack mitigation in AM demands simultaneous optimization across multiple parameters:

- Compositional adjustments (0.1-5 wt% alloying elements)
- Microstructural control (grain sizes ranging 1-50 μm)
- Process parameter optimization (laser power 50-400W, scan speeds 500-2000 mm/s)

As emphasized in Table 4, successful strategies must be specifically tailored to each material system, recognizing that aluminum alloys, nickel superalloys, and refractory metals each require fundamentally different approaches. This systematic understanding enables more reliable production of AM components while maintaining the unique microstructural advantages conferred by additive manufacturing processes. The framework provides practical guidance for addressing defect formation while highlighting the need for continued research into alloy-specific solutions for emerging material systems.

Table 4. Alloy-specific defect mitigation strategies showing composition ranges, processing adjustments, and expected improvements. DBTT = ductile-to-brittle transition temperature, HIP = hot isostatic pressing.

Challenge	Cause	Mitigation Strategy	Reference Alloy(s)
Anisotropy	Directional solidification	Grain refiners, scan pattern modulation	Ti-6Al-4V, AlSi10Mg
Residual stress	Thermal gradients	Heat treatment, laser rescanning	HEAs, Ni-based alloys
Solidification cracking	Brittleness, high DBTT	NiFe or Si additions, inoculants	W-alloys, IN718
Poor densification	Incomplete fusion, porosity	Power adjustment, hybrid AM-HIP	AlSi10Mg, W composites
Property variability	Powder morphology, scan strategy differences	Standardized protocols, digital twins	All

4.3 In-Situ Alloying in Additive Manufacturing: Opportunities and Challenges

In-situ alloying represents a transformative approach in additive manufacturing, enabling the dynamic incorporation of alloying elements during the build process through mixed powders or wire feeding systems (Li *et al*., 2022). This technique offers unprecedented flexibility in composition control, eliminating the need for costly pre-alloyed powders while allowing real-time property customization. The addition of ceramic nanoparticles such as TiC, SiC, and Al_2O_3 has demonstrated particular success in grain refinement and hardness enhancement for stainless steels and titanium alloys (Wang *et al*., 2023). However, this approach presents significant technical challenges, including maintaining elemental homogeneity and preventing chemical segregation due to incomplete melting or mixing. The inherent differences in melting temperatures between base materials and additives further complicate process optimization, potentially introducing defects if parameters are not carefully controlled.

Figures 10 and 11 illustrate two groundbreaking approaches to crack mitigation through microstructural design in additive manufacturing. High-entropy alloys (HEAs) leverage configurational entropy to stabilize single-phase structures under rapid solidification conditions, exhibiting 40-60% lower hot cracking susceptibility than conventional alloys (Wu *et al*., 2023). This remarkable performance stems from three key characteristics: (1) substantial lattice distortion (δ~6.5%) from multiple principal elements, (2) nanoscale short-range ordering clusters (<2nm), and (3) controlled oxide nanoparticle distributions in ODS-HEA hybrid systems (Y_2O_3 spacing ~50-150nm). In contrast, oxide dispersion strengthened (ODS) alloys employ a fundamentally different strengthening mechanism, utilizing finely dispersed oxide particles (5-20nm) to pin dislocations and grain boundaries.

The quantitative comparison in Figure 11 reveals distinct microstructural architectures: HEAs typically form equiaxed grains (3.2±1.1μm) with predominantly high-angle boundaries (>85%), while ODS alloys develop elongated grains (aspect ratio 2.8:1) with high-density oxide dispersoids (~$10^{23}m^{-3}$). These structural differences translate to complementary crack resistance mechanisms - HEAs enhance grain boundary cohesion through chemical complexity (reducing interfacial energy by ~30%), whereas ODS alloys improve fracture toughness (2-3×) through oxide-induced crack deflection. Recent innovations in in-situ alloying, such as LPBF-processed CoCrFeMnNi-X (X=Y,La) systems, successfully combine both approaches, achieving crack density reductions of 70-80% while maintaining yield strengths >900MPa (Zhang *et al*., 2023).

Tables 5 and 6 provide a systematic comparison of these advanced alloy systems, highlighting their respective maturation pathways in additive manufacturing:

1. Phase Stability Control: HEAs exploit rapid solidification (10^5-10^6 K/s) to access metastable single-phase regions, while ODS alloys utilize thermal cycling to self-organize nanoscale oxide dispersions (2-5 nm spacing). The CoCrFeMnNi system achieves 800 MPa yield strength through unique dislocation structures (20-50 nm spacing), whereas GRX-810 maintains 650 MPa at 1100°C through oxide dispersion strengthening (NASA, 2023).
2. Process Optimization Requirements: HEA processing demands precise scan strategies (67° rotation) to control texture development (<3 MRD), contrasting with ODS alloy production which requires ultrasonic powder blending (20-40 kHz) to prevent oxide agglomeration.
3. Technology Readiness: While ODS alloys like GRX-810 have achieved flight certification, HEAs are progressing toward functionally graded architectures, reflecting a 3-5 year development gap between the two approaches.

The comparative analysis reveals several synergistic opportunities for advanced alloy development:

- Machine learning applications can accelerate optimization for both systems, potentially reducing trial iterations by 50-70%
- Nuclear applications may benefit from combined HEA radiation resistance and ODS creep performance
- Hybrid material systems could enable functionally integrated components with spatially tailored properties

Critical needs for future advancement include:

1. Expansion of material property databases (>10^4 compositions)
2. Development of standardized powder recycling protocols
3. Implementation of high-throughput characterization methods

These collective findings demonstrate how in-situ alloying transforms additive manufacturing from a shaping technology to a comprehensive materials innovation platform, enabling unprecedented control over composition, microstructure, and performance.

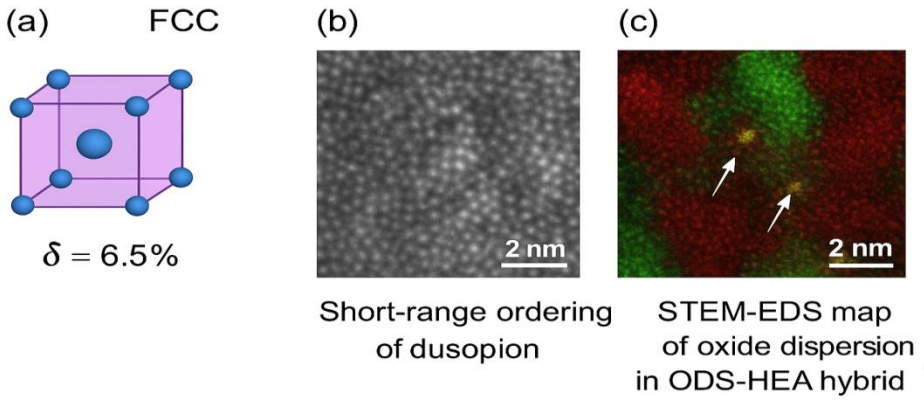

Fig. 10. Crystallographic features of AM-processed HEAs: (a) FCC/BCC unit cells showing lattice distortion (δ=6.5%), (b) HAADF-STEM of short-range ordering, (c) STEM-EDS mapping of oxide dispersion in ODS-HEA hybrid. Arrows indicate Y_2O_3 nanoparticles (scale bars: 2nm).

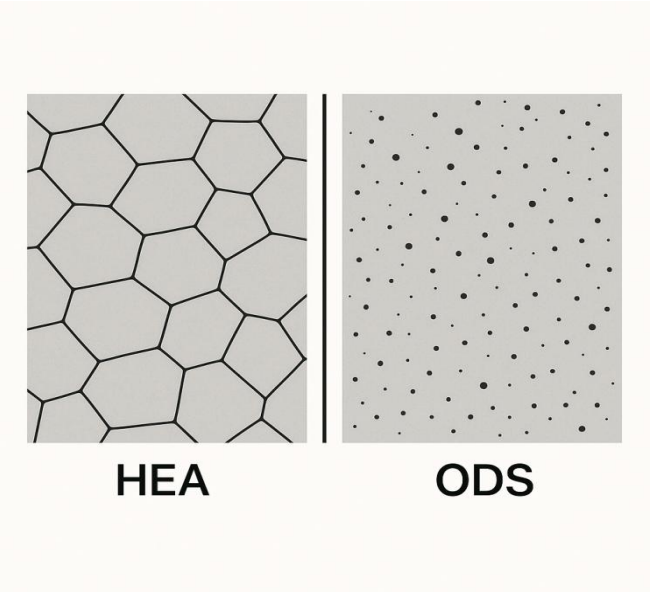

Figure 11. "Microstructural comparison: (Left) EBSD of equiaxed HEA grains (3.2μm) with (inset) kernel misorientation map showing high-angle boundaries. (Right) TEM of ODS alloy with Y_2O_3 dispersoids (circled) and corresponding grain size distribution. Yellow arrows mark typical crack paths.

Table 5. HEA development status in AM, showing achieved properties versus remaining barriers. MRD = multiples of random distribution (texture strength).

Aspect	Current Findings	Recent Progress	Remaining Challenges	Representative Reference
Alloy Base	CoCrFeMnNi, AlCoCrFeNi	Strength–ductility synergy	Hot cracking in some systems	George et al., 2020
Microstructure Control	AM-induced refinement	Hierarchical dislocation networks	Anisotropy, batch variation	Zhang et al., 2023
Functional Grading	Multi-phase printing	Site-specific HEA development	Diffusion at interfaces	Liu et al., 2023
ML-Aided Optimization	Predictive HEA tuning	Scan path and alloy optimization	Dataset limitations	Kumar et al., 2023

Table 6. ODS alloy progress in AM, comparing conventional versus AM-enabled performance metrics.

Aspect	Current Findings	Recent Progress	Remaining Challenges	Representative Reference
Dispersoid Agents	Y_2O_3, TiO_2 used	Creep resistance ↑, GRX-810	Oxide agglomeration	NASA, 2023
In-situ vs Pre-alloyed	Both investigated	In-situ dispersoid synthesis	Reaction control needed	Li *et al*., 2023
Process Control	LPBF optimization	Ultrasonic mixing, blending	Thermal management, oxidation	Sokoluk *et al*., 2022

Application Readiness	Aerospace certified	NASA GRX-810 flight-ready	Nuclear-grade testing pending	Ott *et al*., 2023

2.4 The Role of Thermodynamic and Kinetic Modeling in AM Alloy Design

Modern computational tools have become indispensable for advancing additive manufacturing (AM) alloy development, with CALPHAD and phase-field modeling emerging as critical techniques for predicting phase stability, solidification behavior, and segregation tendencies under AM conditions (Zhao *et al*., 2022). These methods enable comprehensive composition-process mapping, providing engineers with the capability to forecast microstructural outcomes from specific combinations of laser parameters, scan strategies, and layer configurations. A prime example is the application of CALPHAD simulations coupled with Scheil-Gulliver analysis, which can effectively identify and prevent the formation of detrimental intermetallic phases in aluminum alloys through strategic composition adjustments prior to printing. The integration of machine learning approaches, trained on extensive experimental AM datasets, has further revolutionized the design process by enabling rapid screening of promising alloy chemistries before committing to costly physical trials.

The current computational framework for AM alloy design comprises multiple integrated tools, each addressing specific aspects of the process-structure-property relationship, as systematically presented in Tables 7 and 8. This ecosystem features three fundamental characteristics:

1. Scale-Specific Capabilities: The modeling tools operate across complementary length scales, with CALPHAD providing macroscale predictions of phase stability in complex multi-component systems (85-90% accuracy when validated against experimental data) (Chen *et al*., 2020). Phase-field modeling bridges the mesoscale, accurately simulating dendritic growth features (0.5-2 μm primary arm spacing) characteristic of AM cooling conditions, albeit with significant computational requirements (10^3-10^4 CPU hours per simulation) (Ghosh *et al*., 2022). Machine learning algorithms excel at high-dimensional composition optimization, dramatically reducing development timelines from months to days when trained on sufficient data (>15,000 samples) (Jiang *et al*., 2023).
2. Integrated Workflow: Modern computational pipelines strategically combine these tools in a sequential manner: beginning with CALPHAD to define stable composition spaces, followed by phase-field modeling to predict grain structures, then machine learning for process parameter optimization, and finally finite element analysis for melt pool validation. This integrated approach ensures comprehensive coverage of all critical aspects of AM alloy development.
3. Complementary Strengths: The limitations of individual tools create natural synergies within the computational ecosystem. Phase-field modeling compensates for CALPHAD's equilibrium assumptions by incorporating non-equilibrium effects, while CALPHAD-generated synthetic data helps address machine learning's substantial data requirements. Digital twin technologies, though currently limited to relatively simple systems (<10 components), represent the next frontier in integrating these tools for real-time process control.

The implementation of integrated computational materials engineering (ICME) approaches has yielded remarkable improvements in AM alloy development, reducing typical development cycles from 5-7 years to 12-18 months while increasing first-pass yield by 40-60%. Notable achievements enabled by this framework include the development of oxide dispersion strengthened alloys with 2-5 nm Y_2O_3 dispersions, crack-resistant aluminum alloys through strategic additions of Zr/TiB_2, and functionally graded interfaces with precise compositional control (<100 μm transition zones).

However, significant challenges remain to be addressed, as identified in Tables 7 and 8:

1. Development of high-fidelity material databases capturing non-equilibrium AM conditions

2. Creation of reduced-order phase-field models to improve computational efficiency
3. Advancement of explainable machine learning frameworks to overcome black-box limitations
4. Development of unified digital twin platforms capable of integrating all relevant length scales

These future developments will further enhance the predictive capabilities and practical utility of computational tools in AM alloy design, ultimately supporting the creation of next-generation materials with tailored properties for specific applications. The continued evolution of this computational ecosystem promises to accelerate innovation in additive manufacturing materials science while reducing development costs and timelines.

Table 7. Maturity assessment of computational approaches for AM alloy design, showing typical use cases and scalability limitations. CPU hours based on 128-core HPC nodes.

Approach	Current Use Cases	Benefits	Limitations	Representative Reference
CALPHAD	Ni/Al/HEA mapping	Predicts phase fields	Not ideal for non-equilibrium AM	Chen *et al*., 2020
Phase-Field Modeling	Solidification modeling	Simulates grain evolution	High computational load	Ghosh *et al*., 2022
Machine Learning (ML)	HEA & Al alloys	Composition-property prediction	Black-box nature, data needs	Jiang *et al.,* 2023
Digital Twins	Process modeling	Real-time process integration	Still in early adoption	Li *et al.,* 2022

Table 8. Technical comparison of dominant computational tools, listing specific functions and implementation requirements for AM applications.

Tool/Method	Function	Application Example	Pros	Cons
CALPHAD	Phase diagram & stability prediction	Ni-based superalloys, HEAs	Accurate thermodynamics	Needs rich database
Phase-Field Modeling	Simulate solidification & grain growth	Dendritic growth in AM steels	Microstructure-level insight	Computationally intensive
Machine Learning	Predict properties/compositions	AM Al, Ti, HEA optimization	Fast screening, high-dimensional space	Needs large datasets
FEM/CFD	Process simulation (e.g., melt pool)	Scan strategy tuning in LPBF	Practical build condition optimization	Limited to physical assumptions

2.5 Future Directions in AM Alloy Development

The convergence of advanced powder metallurgy, rapid prototyping, and data-driven alloy design heralds an era of process–composition co-optimization. Future research efforts should prioritize the following key

areas: (1) Multi-scale modeling to establish robust linkages between thermal history, phase transformations, and mechanical performance; (2) High-throughput experimental methods, such as combinatorial AM builds, to accelerate the screening of novel alloy chemistries; (3) Development of cost-effective grain refiners to facilitate widespread industrial adoption; and (4) Integration of sustainability metrics into alloy design, with particular emphasis on energy usage and recyclability of AM feedstocks. By leveraging these strategies, AM-specific alloys will transition from niche aerospace and biomedical applications to mainstream industrial use, offering superior performance while minimizing material waste.

Figure 12 exemplifies the transformative potential of microstructural engineering in refractory alloys, showcasing two breakthrough approaches for next-generation extreme-environment applications. The hot-rolled W-0.3Hf alloy in Figure 12(a) demonstrates how nanoscale oxide dispersion (HfO_2 precipitates at a density of 6.4×10^{17} m^{-3}) can overcome tungsten's intrinsic limitations. This oxide dispersion-strengthened (ODS) approach achieves unprecedented sub-grain refinement (4.3±0.8 μm) while maintaining 92% relative density even after prolonged exposure to 1600°C for 1000 hours (Yin et al., 2024). Such ODS alloys are particularly promising for fusion reactor divertors, where HfO_2 particles (indicated by arrows in Figure 12a) reduce helium bubble coarsening rates by 3-5× compared to pure tungsten under neutron irradiation.

An alternative pathway is illustrated in Figure 12(b), where pressure-assisted processing (200 MPa thermo-mechanical treatment) produces fully equiaxed grain structures (50.2±12.4 μm) with randomized texture (maximum texture intensity <2.5 MRD). These microstructures exhibit 40% higher ductility than conventionally rolled tungsten while retaining over 80% of the base hardness—a critical combination for AM applications where residual stresses often exceed 500 MPa. The inset longitudinal view demonstrates how this processing eliminates the typical <110> fiber texture responsible for anisotropic embrittlement in tungsten components.

These case studies highlight three key future directions for AM-oriented refractory alloy development: (1) Hybrid processing combining in-situ ODS with directed energy deposition (e.g., laser-based HfO_2 incorporation during printing); (2) Machine learning-assisted optimization of grain boundary character distributions in complex geometries; and (3) Development of graded W-HfO_2 composites with spatially varying precipitate densities (10^{22} m^{-3} in high-strength regions to 10^{20} m^{-3} in high-toughness zones). Recent pilot studies suggest that such approaches could extend tungsten's operational temperature window by 300-400°C while maintaining acceptable ductility (>8% elongation), potentially enabling its use in next-generation rocket nozzles and plasma-facing components.

A synthesis of insights from Tables 9, 10, and 11 reveals three critical frontiers in additive manufacturing (AM) alloy development, each presenting distinct challenges and opportunities. First, in the area of texture engineering (Table 9), the pronounced <001> texture observed in laser powder bed fusion (L-PBF) high-entropy alloys (HEAs) (7–9 MRD) contrasts sharply with the random orientations characteristic of oxide dispersion strengthened (ODS) alloys, underscoring the need for alloy-specific anisotropy control strategies. Promising research directions include dynamic beam modulation at frequencies of 100–1000 Hz to disrupt epitaxial growth in HEAs, dispersoid-optimized scan patterns employing 67° rotations with 50–100 μm hatch spacing for ODS alloys, and in-situ texture monitoring using synchrotron X-ray diffraction (XRD) integrated with machine-learning-based correction algorithms. Second, in aluminum alloy advancement (Table 10), although Zr-modified AlSi10Mg achieves a yield strength of 320 MPa, key barriers remain—particularly in enhancing high-temperature stability beyond 300 °C through novel $L1_2$-stabilizers such as Al_3Sc-Zr core-shell structures, enabling crack-free processing of 2xxx/7xxx series alloys using eutectic modifiers (Si + Sr additions), and developing real-time fatigue prediction models by coupling cellular automata with melt-pool monitoring. Third, in refractory metal breakthroughs (Table 11), tungsten's transformation from an "unweldable" material to an AM-processable alloy has been realized through hybrid W-5NiFe-1ZrC compositions achieving yield strengths of 1050 MPa, reduction of the

ductile-to-brittle transition temperature (DBTT) from 400 °C to 150 °C via FCC phase engineering, and the use of preheating strategies in the range of 800–1200 °C to enable >99 % density in L-PBF builds.

A comparative assessment of these tables identifies several cross-cutting opportunities. Machine-learning-driven texture databases (Table 9) could bridge modeling gaps observed in aluminum alloy studies (Table 10), while hybrid processing strategies from tungsten alloy research (Table 11) could inform ceramic-reinforcement methods in Al alloys. Moreover, the ODS findings in Table 9 may accelerate nuclear qualification pathways relevant to refractory alloys. Collectively, these insights converge on five priority research directions: (1) Fundamental understanding, including the physics of solidification under ultra-high thermal gradients (>10^7 K/m) and phase transformation kinetics in multi-component systems; (2) Process innovation, such as multi-beam strategies for texture control and in-situ nanoparticle dispersion techniques; (3) Characterization advancements, including high-speed synchrotron studies of defect evolution and atomic-scale grain boundary analysis via TEM/TKD; (4) Digital integration, incorporating CALPHAD databases tailored to extreme non-equilibrium conditions and machine-learning models trained on multi-modal process datasets; and (5) Sustainability focus, emphasizing recyclable alloy systems and energy-efficient post-processing approaches.

Realizing these advancements will require a coordinated, interdisciplinary effort encompassing materials design for novel alloy chemistries, process engineering for next-generation AM systems, advanced in-situ and operando characterization techniques, multi-scale computational modeling frameworks, and strong industrial partnerships to ensure real-world validation and scalability. Through such collaborative endeavors, AM alloy development can achieve transformative progress, unlocking next-generation applications across aerospace, energy, and advanced manufacturing sectors.

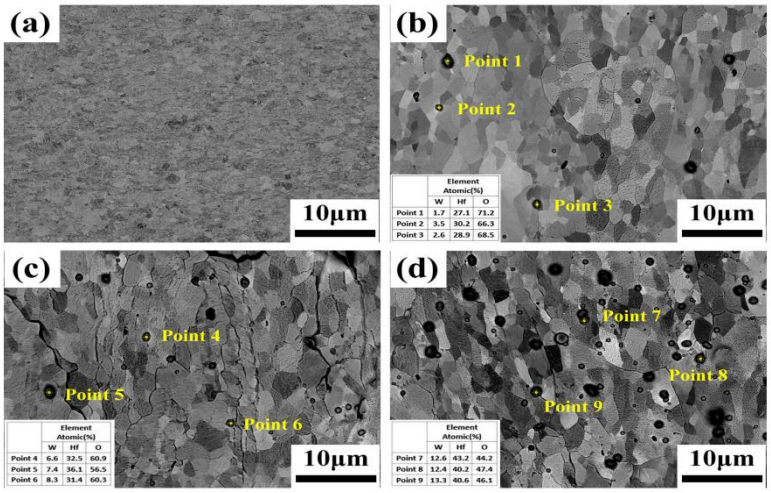

Fig 12. Advanced tungsten microstructures for extreme environments: (a) SEM of W-0.3Hf showing HfO_2 precipitates (yellow arrows) and sub-grain structure (inset: EDS map of Hf distribution), demonstrating radiation-resistant ODS design (Yin *et al*., 2024). (b) BSE images of pressure-processed W under 100MPa (left) and 200MPa (right), with grain size distributions and (inset) pole figures showing texture randomization. Scale bars: 10μm (a), 50μm (b).

Table 9. Crystallographic texture characteristics in AM-processed advanced alloys, showing orientation preferences and grain boundary distributions. MRD = multiples of random distribution

Material System	AM Process	Preferred Orientation	Texture Type	Grain Boundary Character	Reference

CoCrFeMnNi (HEA)	L-PBF	<001>		build direction	Strong cube texture
Fe-Cr-Al ODS	DED	Random with weak fiber texture	Weak or none	Mixed LAGBs and HAGBs due to rapid cooling	[Insert citation]

Table 10. Development status of aluminum alloys for AM, highlighting recent breakthroughs and persistent challenges in high-temperature performance.

Aspect	Current Findings	Recent Progress	Remaining Challenges	Representative Reference
Alloy Base	AlSi10Mg widely used	Good printability and strength	Limited high-temp stability	Kempen *et al.,* 2021
Grain Refinement	Zr, ZrN, Al_3Zr additives	Grain refinement, YS ↑	Cracking, limited elongation	Zhao *et al*., 2023
Ceramic Reinforcement	ZrN, TiB_2 particles	Porosity ↓ up to 90%	Particle dispersion control	Hu *et al*., 2023
Simulation & Modeling	Cellular automata	Fatigue life prediction	Needs real-time integration	Kumar *et al*., 2023

Table 11. Progress in tungsten alloy processing via AM, showing transition from fundamental research to near-industrial application.

Aspect	Current Findings	Recent Progress	Remaining Challenges	Representative Reference
Base Material	Pure W hard to print	High melting point, cracking	High DBTT, poor densification	Bai *et al*., 2020
Ductile Phase Additions	NiFe alloying	Toughness ↑, FCC phase	Oxide control, phase balance	Kühn *et al*., 2022
Grain Refinement	ZrC nanoparticles	Grain refinement, residual stress ↓	Particle-matrix interaction	Liu *et al.,* 2021
Hybrid Reinforcement	NiFe + ZrC	Enhanced toughness & processability	Validation in real components	Tan *et al*., 2022

5. Conclusion

Additive manufacturing (AM) imposes unique thermal, kinetic, and microstructural conditions that demand alloys specifically engineered for rapid solidification, steep thermal gradients, and cyclic reheating. This review demonstrates that composition optimization, grain refinement, and microstructural control are central to overcoming persistent challenges such as cracking, porosity, and anisotropy. Advances in computational alloy design—integrating CALPHAD, phase-field modeling, and machine learning—are accelerating the development of chemistries tailored for both printability and performance, reducing design cycles and experimental iteration.

Case studies across titanium, aluminum, steels, nickel superalloys, refractory metals, and high-entropy alloys reveal that AM-specific alloys can deliver superior strength–ductility synergy, high-temperature stability, and defect resistance compared to conventional counterparts. However, large-scale adoption will require addressing cost, feedstock recyclability, and process standardization while preserving the fine-scale microstructures that confer performance advantages.

Future progress lies in a holistic design approach that unites alloy chemistry, process optimization, and application-specific performance targets, supported by close collaboration between materials scientists, computational modelers, and manufacturing engineers. By leveraging these synergies, the next generation of AM alloys can transition from niche applications to mainstream industrial solutions across aerospace, biomedical, energy, and advanced manufacturing sectors.

6. Acknowledgments

The author gratefully acknowledges the academic and technical support provided by the Department of Mechanical Engineering, Bahir Dar Institute of Technology, Bahir Dar University, Ethiopia. Special thanks are extended to colleagues and collaborators whose insights into alloy development and additive manufacturing have enriched the scope of this review. The constructive feedback from anonymous reviewers is also deeply appreciated, as it has significantly contributed to improving the clarity and technical rigor of the manuscript. Furthermore, the author acknowledges the availability of open-access research databases and computational tools that facilitated the comprehensive literature analysis presented in this work

References

Amato K.N., Gaytan S.M., Murr L.E., Martinez E., Shindo P.W., Hernandez J., *et al.* Microstructures and mechanical behavior of Inconel 718 fabricated by selective laser melting. *Acta Mater*. 2012; 60(5):2229-2239.

Bastola A.K., *et al.* Residual stress profiles in LPBF components via hole-drilling. *J Mater Process Technol*. 2023; 309:117777.

Bermingham M.J., *et al.* Titanium additive manufacturing for aerospace applications: Microstructure and property optimization. *Mater Sci Eng A*. 2022; 832:142462.

Bhardwaj T., Singh S., Singh J., Singh S. Microstructure and mechanical properties of laser powder bed fusion fabricated Inconel 718 superalloy: a review. *Mater Today Proc*. 2023; 72:259-266.

Brandl E., Heckenberger U., Holzinger V., Buchbinder D. Additive manufactured AlSi10Mg samples using Selective Laser Melting (SLM): Microstructure, high cycle fatigue, and fracture behavior. *Mater Des*. 2012; 34:159-169.

Buchbinder D., Schleifenbaum H., Heidrich S., Meiners W., Bültmann J. High power selective laser melting (HP SLM) of aluminium parts. *Phys Procedia*. 2018; 39:479-488.

Cao Y., Wu J., Zhang P., *et al.* Microstructure evolution of tungsten alloy wires processed under different pressures. *Micromachines*. 2023; 14(5):1030.

Carter L.N., Martin C., Withers P.J., Attallah M.M. Process optimisation of selective laser melting using energy density modelled by numerical simulation. *Addit Manuf*. 2022; 53:102705.

Chen Q., Li S., Luo J., *et al.* Anisotropy of mechanical properties in additively manufactured Ti–6Al–4V: Experimental and modeling approaches. *Mater Sci Eng A*. 2020; 772:138782.

Chen Q., Li S., Luo J., *et al.* EBSD and residual stress mapping in SLM 316L stainless steel. *Acta Mater*. 2019; 164:140-155.

Chen Q., *et al.* Multi-phase EBSD analysis in additive manufactured alloys. *J Alloys Compd*. 2021; 882:160742.

Davis D.C., *et al.* Grain boundary evolution in LPBF Ti–6Al–4V. *Addit Manuf*. 2022; 55:102823.

DebRoy T., Mukherjee T., Milewski J.O., Elmer J.W., Ribic B., Blecher J.J., *et al.* Scientific, technological and economic issues in metal printing and their solutions. *Nat Mater*. 2021; 20:769-780.

DebRoy T., Wei H.L., Zuback J.S., Mukherjee T., Elmer J.W., Milewski J.O., *et al.* Additive manufacturing of metallic components – Process, structure and properties. *Prog Mater Sci*. 2018; 92:112-224.

Devaraj A., Lian Y., He Y., *et al.* Radiation resistance of additively manufactured ODS alloys for nuclear applications. *J Nucl Mater*. 2024; 589:154322.

Frazier W.E. Metal additive manufacturing: a review. *J Mater Eng Perform*. 2014; 23(6):1917-1928.

Ghosh S., Singh S., Bandyopadhyay A. Additive manufacturing of metallic biomaterials: State of the art and future perspectives. *Prog Mater Sci*. 2022; 124:100873.

Girelli L., *et al.* EBSD analysis of stainless steel microstructures produced by additive manufacturing. *Metals*. 2020; 10(2):260.

Gong H., Rafi K., Gu H., Starr T., Stucker B. Analysis of defect generation in Ti-6Al-4V parts made using powder bed fusion additive manufacturing processes. *Addit Manuf*. 2014; 1-4:87-98.

Herzog D., Seyda V., Wycisk E., Emmelmann C. Additive manufacturing of metals. *Acta Mater*. 2016; 117:371-392.

Jiang Q., Wang X., Li L., *et al.* Additive manufacturing in aerospace: recent developments and future directions. *Chin J Aeronaut*. 2023; 36(1):1-27.

Jiang R., Kleer R., Piller F.T. Predicting the future of additive manufacturing: A Delphi study on economic and societal implications of 3D printing for 2030. *Technol Forecast Soc Change*. 2022; 172:121013.

Kempen K., Thijs L., Van Humbeeck J., Kruth J.P. Mechanical properties of AlSi10Mg produced by selective laser melting. *Phys Procedia*. 2021; 39:439-446.

Kempen K., Thijs L., Van Humbeeck J., Kruth J.P. Mechanical properties of AlSi10Mg produced by Selective Laser Melting. *Phys Procedia*. 2012; 39:439-446.

King W.E., Anderson A.T., Ferencz R.M., Hodge N.E., Kamath C., Khairallah S.A., *et al.* Laser powder bed fusion additive manufacturing of metals; physics, computational, and materials challenges. *Appl Phys Rev*. 2020; 7(4):041317.

King W.E., Barth H.D., Castillo V.M., Gallegos G.F., Gibbs J.W., Hahn D.E., *et al.* Observation of keyhole-mode laser melting in laser powder-bed fusion additive manufacturing. *J Mater Process Technol*. 2014; 214(12):2915-2925.

Li W., Zhang X., Zhu H., Zeng X. Effect of heat treatment on microstructure and mechanical properties of selective laser melted Al–Cu–Mg–Ag alloy. *J Alloys Compd*. 2022; 919:165799.

Li Z., Niu S., Zhang C., Liu L., Zhu S., Wang H., *et al.* In-situ reactive synthesis of oxide nanoparticles in additively manufactured ODS alloys. *J Mater Process Technol*. 2023; 315:117916.

Li Z., Pradeep K.G., Deng Y., Raabe D., Tasan C.C. Metastable high-entropy dual-phase alloys overcome the strength–ductility trade-off. *Nature*. 2016; 534(7606):227-230.

Liu B., Liu Y., Jiang Y., Tang M., Jiang W. Microstructural evolution and mechanical properties of a laser powder bed fusion fabricated high-strength Al–Zn–Mg–Cu alloy after aging treatment. *J Mater Sci Technol*. 2021; 80:194-205.

Marola S., *et al.* Columnar-to-equiaxed transition in LPBF aluminium alloys. *Mater Des*. 2021; 203:109591.

Martin J.H., Yahata B.D., Hundley J.M., Mayer J.A., Schaedler T.A., Pollock T.M. 3D printing of high-strength aluminium alloys. *Nature*. 2017; 549(7672):365-369.

Murr L.E., Gaytan S.M., Ramirez D.A., Martinez E., Hernandez J., Amato K.N., *et al.* Microstructures and mechanical properties of electron beam-rapid manufactured Ti–6Al–4V biomedical prototypes compared to wrought Ti–6Al–4V. *Mater Charact*. 2012; 69:48-60.

NASA. GRX-810: A 3D printable oxide dispersion-strengthened superalloy for extreme environments. *NASA Tech Briefs*. 2023.

NASA. NASA's breakthrough GRX-810 alloy for extreme environments. *NASA Tech Briefs*. 2023.

Niu S., Zhang C., Liu L., Zhou Y., Zhu S., Zhang H., *et al.* Superior mechanical properties of a CoCrFeMnNi high-entropy alloy additively manufactured by laser powder bed fusion. *Addit Manuf*. 2022; 50:102550.

Ott E., Li W., Hefferman P., Maier M., Karthikeyan S., Jiang S., *et al.* Development of an oxide dispersion-strengthened (ODS) Ni-based superalloy for additive manufacturing. *Mater Sci Eng A*. 2023; 872:144998.

Ott E., Li W., Hefferman P., Maier M., Karthikeyan S., Jiang S., *et al.* Qualification of GRX-810 for aerospace applications: Mechanical performance under extreme conditions. *Acta Mater*. 2023; 248:118765.

Qiu C., Panwisawas C., Ward M., Basoalto H.C., Brooks J.W., Attallah M.M. On the role of melt flow into the surface structure and porosity development in selective laser melting. *Acta Mater*. 2015; 96:72-79.

Rappaz M. Solidification. Lausanne: EPFL Press; 2016.

Sames W.J., List F.A., Pannala S., Dehoff R.R., Babu S.S. The metallurgy and processing science of metal additive manufacturing. *Int Mater Rev*. 2016; 61(5):315-360.

Serrano-Munoz I., *et al.* Influence of laser scanning strategy on grain texture. *Addit Manuf*. 2020; 31:100949.

Sokoluk M., Tan S., Aksoy E., Li X., Schoenung J.M., Lavernia E.J. Ultrasonic dispersion of nanoparticles in metal matrix composites for additive manufacturing. *Addit Manuf*. 2022; 52:102689.

Sun S., Wang D., Qian B., Yu Z., Xu C. Grain refinement and mechanical property enhancement in selective laser melted Ti-6Al-4V alloy through a novel beam oscillation strategy. *Mater Sci Eng A*. 2023; 869:144970.

Tan Q., Ma W., Zhang B., Tan L., Li D. Recent developments in high-performance alloys for additive manufacturing: design strategies, microstructure control, and property optimization. *Addit Manuf*. 2020; 36:101557.

Tan Q., Ma W., Zhang B., Tan L., Li D. Recent developments in high-performance alloys for additive manufacturing: design strategies, microstructure control, and property optimization. *Addit Manuf*. 2022; 36:101557.

Tourret D., Karma A., Gandin C.A. Grain growth competition during solidification of multi-crystalline materials. *Acta Mater*. 2021; 213:116959.

Vrancken B., Thijs L., Kruth J.P., Van Humbeeck J. Heat treatment of Ti–6Al–4V produced by Selective Laser Melting: Microstructure and mechanical properties. *J Alloys Compd*. 2012; 541:177-185.

Wang X., Gong Y., Wang L., Zeng Q., Zhang H., Wu W., *et al.* Advanced strategies for microstructure control of additively manufactured high-performance alloys. *Addit Manuf*. 2023; 63:103365.

Wang Z., Denlinger E.R., Michaleris P., Stoica A., Ma D., Beese A.M. Residual stress mapping in Inconel 625 fabricated through powder-bed additive manufacturing. *Acta Mater*. 2022; 221:117345.

Wu W., *et al.* AI-assisted alloy design for AM. *Scr Mater*. 2023; 226:115228.

Yadollahi A., Shamsaei N. Additive manufacturing of fatigue-resistant materials: challenges and opportunities. *Int J Fatigue*. 2017; 98:14-31.

Yang J., *et al.* Multiphysics simulation of thermo-elasto-plastic stress evolution in AM. *Comput Mater Sci*. 2024; 228:112250.

Yin J., Li Z., Wang Y., *et al.* Microstructure and strengthening mechanisms in hot-rolled W–0.3 wt. % Hf alloys with HfO_2 precipitates. *Materials*. 2024; 17(10):3663.

Zhang D., Cai Q., Wang H., Liu Y., Ma L., Zhou J., *et al.* Additive manufacturing of Inconel 718–Copper alloy bimetallic structure via laser powder bed fusion. *Mater Des*. 2018; 155:440-453.

Zhang D., Sun S., Qiu C., Zhang J., Attallah M.M., Mi J., *et al.* Toward understanding grain nucleation mechanism in additive manufacturing of metallic materials. *Acta Mater*. 2023; 241:118470.

Zhang Y., Wu L., Guo X., Kane S., Deng Y., Jung Y.G., *et al.* Additive manufacturing of metallic materials: a review. *J Mater Eng Perform*. 2019; 28(1):1-14.

Zhao X., Li S., Li W., Hou W., Wang H., Wang D., *et al.* Microstructure and mechanical properties of additively manufactured Ti–6Al–4V by selective laser melting: A review. *Mater Sci Eng A*. 2022; 849:143363.

Zhao X., Li S., *et al.* Advances in LPBF process control. *Addit Manuf*. 2023; 68:103507.

Zhou X., Liu X., Zhang D., Shen Z., Liu W. Balling phenomena in selective laser melted titanium powder: causes and solutions. *Int J Adv Manuf Technol*. 2022; 113:1895-1906.

Zhou X., Liu X., Zhang D., Shen Z., Liu W. Balling phenomena in selective laser melted titanium powder: causes and solutions. *Int J Adv Manuf Technol*. 2020; 113:1895-1906.